Subproject F2.2

Reaction kinetics of nanostructured SOFC cathodes

Principle Investigators: Ellen Ivers-Tiffée

CFN-Financed Scientists: Jan Hayd (BAT IIa, 9 months), Thorsten Chrobak (TVÖD E13, 10 months)

Further Scientists: Steffen Busché, Jochen Joos, Dr. André Weber (IWE), Levin Dieterle (Laboratorium für Elektronenmikroskopie, KIT)

Institut für Werkstoffe der Elektrotechnik (IWE)
Karlsruhe Institute of Technology (KIT) (until Oct. 2009: Universität Karlsruhe (TH))

Reaction kinetics of nanostructured SOFC cathodes

1. Introduction

The electrochemical efficiency of solid oxide fuel cells (SOFC) at reduced operating temperatures can significantly be increased by the application of nanostructured electrodes [1-9]. Both aspects, a reduction of operating temperatures along with an increased electrochemical performance, are crucial for SOFC-based Auxiliary Power Unit (APU) systems providing electrical energy in automobiles, ships and aircrafts. The demand for high power densities arises from the limited space in automotive applications. The reduction of operating temperatures ($T < 700$ °C) allows short start-up times of APU systems. For the realization of these goals an improvement of the electrochemically active single cell with special emphasis on the oxygen electrode (cathode) is critical.

In order to do so, it is crucial to understand the reaction kinetics of such nanoscaled cathodes. A thorough understanding is necessary for further optimizing the electrodes in terms of microstructure and material choice. Preliminary work revealed the high performance that can be achieved with nanostructured cathodes, however, a systematic study of the different parameters particle size, porosity, film thickness and material composition has not been performed so far.

In the former projects D5 and D7.2 a novel preparation method for nanostructured layers in association with the Fraunhofer Institute for Silicate Research (ISC), Würzburg, has successfully been implemented. A metal organic deposition (MOD) process facilitates a reproducible preparation of homogeneous, crack-free thin-films with adjustable grain sizes, rendering possible an investigation of the influence of nanoscale structuring on ionic and electronic charge transport processes. In the related joint NSF and DFG research project "Nanoionics" MOD has also been proven to be a versatile chemical route for the fabrication of nanoscaled thin film electrolyte layers made of fluorite type yttria-doped zirconia or gadolinia-doped ceria next to nanoscaled thin film cathodes made of perovskite type (La,Sr)$CoO_{3-\delta}$ or (La,Sr)$MnO_{3-\delta}$.

For a technical application of SOFCs with such nanostructured cathodes, a two-layer electrode structure is required. Firstly, the nanostructured cathode layer has the task of enhancing both the oxygen surface exchange (high surface exchange coefficient k^{δ}) and the oxygen diffusion (high diffusion coefficient D^{δ}). The most promising cathode material with this regard is the perovskite composition (La,Sr)$CoO_{3-\delta}$ (LSC), a mixed ionic-electronic conducting (MIEC) material. For each material composition, an optimum set of parameters cathode thickness, grain size and porosity exists with regard to the electrochemical properties. These can be adjusted via different preparation routes of the MOD process.

Furthermore, a second current collector layer is necessary: This consists of a conventional microstructured layer which must fulfil the requirements of carrying the reactive gases to the cathode (structural requirement) as well as supplying a sufficient number of electrons (high electronic conductivity) that are necessary for the oxygen reduction reaction:

$$1/2\ O_2 + V_O^{\square} + 2\ e^- \rightarrow O_O^x$$

As there are stability problems with zirconia based electrolytes, (La,Sr)$CoO_{3-\delta}$ cathodes are tested and implemented on ceria based electrolytes, such as gadolinia-doped ceria (GCO), only.

2. Sample Fabrication

The nanoscaled thin film cathodes were applied by metal organic deposition. This is a sol-gel based wet chemical route employing propionates of La, Sr and Co as precursors dissolved in propionic acid. The precursors were derived from $La_2(CO_3)_3$, $Co(OH)_2$ and Sr metal by the reaction with propionic acid (in excess) in the presence of propionic acid anhydride separately. To obtain the final

coating sol, the precursors were then dissolved in propionic acid at room temperature in the aimed stoichiometry $La_{0.6}Sr_{0.4}CoO_{3-\delta}$ (LSC). Best results in terms of homogeneous and crack-free thin films were obtained with a solution containing 10 mass% of the resulting oxide. The final composition of the coating sol was measured by inductively coupled plasma-atomic emission spectroscopy (ICP-AES). Our cooperation partner ISC prepared the ready-to-use sol, however the actual fabrication of the thin film cathodes was done at the IWE.
The thin film cathodes were applied onto thin (400 – 800 µm, $d \approx 25$ mm) $Ce_{0.9}Gd_{0.1}O_{1.95}$ (GCO) electrolyte pellets (Daiichi Kigenso Kagaku Kogyo Co. Ltd, Japan) by a single dip coating step with a withdraw rate of 8 cm min^{-1}. In a subsequent drying process at room temperature for 5 minutes, followed by a rapid thermal annealing (RTA) step at 170 °C for 5 minutes, all volatile components were removed from the coating. In a second high temperature step, the actual perovskite phase was formed. In this step, different heating rates, rapid thermal annealing or a slow heating with a heating ramp of $\Delta T = 3$ K min^{-1}, different maximum processing temperatures of $T_{max} = 700$ or 800 °C, and different annealing times of $t_{an} = 0$, 10 and 100 h were applied, resulting in different microstructures of the thin film cathodes.

Table 1: Processing parameters of the high temperature step for sample preparation.

Parameter	Value	Explanation
T_{max}	700 °C, 800 °C	maximum processing temperature
ΔT	3 K min^{-1}, > 200 K min^{-1} (RTA)	heating rate
t_{an}	0 h, 10 h, 100 h	annealing time at T_{max}

3. Results

3.1 Chemical compatibility with electrolyte material

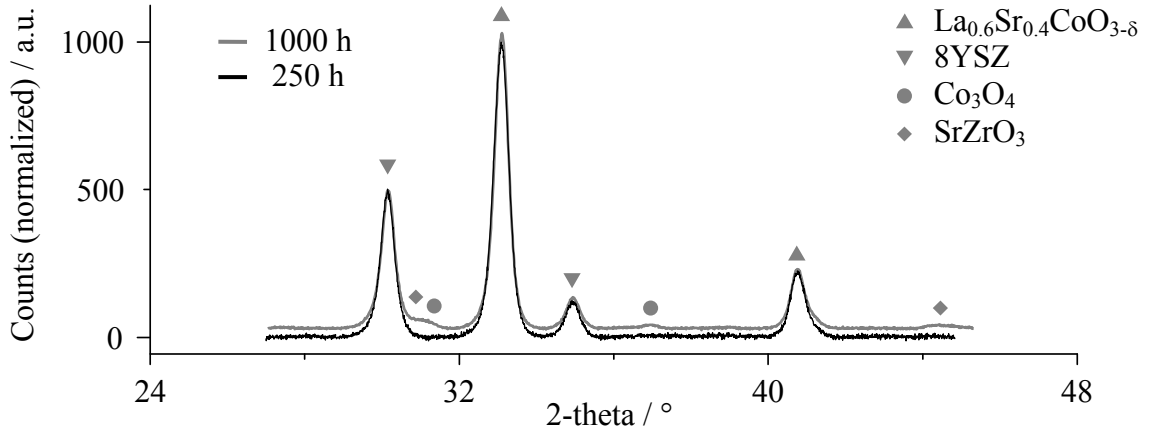

Figure 1. X-ray diffraction pattern (significant angle range) of powder mixtures of $La_{0.6}Sr_{0.4}CoO_{3-\delta}$ and 8YSZ annealed in air at 600 °C for 250 h (black spectrum) and 1000 h (grey spectrum).

As a result of the former projects D5.1 and D5.2, the formation of secondary phases, such as $SrZrO_3$ or Co_3O_4, was identified for LSC type cathodes in combination with zirconia based electrolytes at elevated temperatures [6;10]. However, these studies were limited to temperatures of 700 °C and higher and nothing was known about the chemical compatibility of LSC and YSZ at temperatures below 700 °C. To gain more insight into this, annealing experiments with powders were conducted. Even at 600 °C $SrZrO_3$ and Co_3O_4 formation was observed for powder mixtures of $La_{0.6}Sr_{0.4}CoO_{3-\delta}$ and 8 mol% yttria-doped zirconia (8YSZ) (Tosho Corporation, Japan) after annealing for 1000 h (see Figure 1). As kinetics are slow at this temperature, annealing for 250 h was not sufficient and

only after 1000 h a detectable amount of the secondary phases was formed. Qualitatively similar results were obtained for other stoichiometries such as $La_{0.5}Sr_{0.5}CoO_{3-\delta}$ and $La_{0.7}Sr_{0.3}CoO_{3-\delta}$. Consequently, experiments with zirconia based electrolytes were discontinued and ceria based electrolytes, in particular $Ce_{0.1}Gd_{0.9}O_{1.95}$, were used instead.

3.2 Microstructural and chemical characterization

The resulting microstructures were analyzed by scanning electron microscopy (SEM) (Zeiss 1540XB, Carl Zeiss NTS GmbH) at the Institut für Werkstoffe der Elektrotechnik (IWE) and by transmission electron microscopy (TEM) at the Laboratory for Electron Microscopy (LEM), within the CFN, with a 200 keV Philips CM200 FEG/ST equipped with a field emission gun. Grain sizes were determined from surface SEM micrographs using the image processing software SPIP™ (Image Metrology A/S) and from TEM plan view images using ImageJ (http://rsbweb.nih.gov/ij/). The mean grain-size d_{mean} was calculated as a circle equivalent diameter from the grain area, averaging over at least 288 (SEM) or 120 (TEM) grains. The porosity ε was determined with a FEI Titan3 80-30 transmission electron microscope by means of a high-angle annular dark-field (HAADF) 3D STEM tomography reconstruction of the thin film cathodes using the simultaneous iterative reconstruction technique (SIRT) [11]. This was done for two samples only, as it is rather complex and time consuming. X-ray diffraction (XRD) (Siemens D5000, Bruker-AXS) was used to investigate crystallization and chemical homogeneity. The setup was operated in the grazing incidence mode with a tube angle of 1.5° using a copper radiation source ($Cu_{K\alpha 1}$, λ = 0.15406 nm).

X-ray diffraction analysis confirmed phase pure $La_{0.6}Sr_{0.4}CoO_{3-\delta}$ formation for the thin film cathodes [12;13]. An X-ray diffraction pattern of a nanoscaled thin film cathode processed at 700 °C (ΔT = 3 K min^{-1}) and without further annealing is plotted in Figure 2. This shows, that a temperature treatment at 700 °C is sufficient for the formation of phase pure LSC derived by MOD. The rather broad LSC related peaks result from the nanoscaled grain size. Secondary phases, e.g. reaction products between LSC and GCO, were not detected, which is in agreement with [14;15], as they are not expected to form.

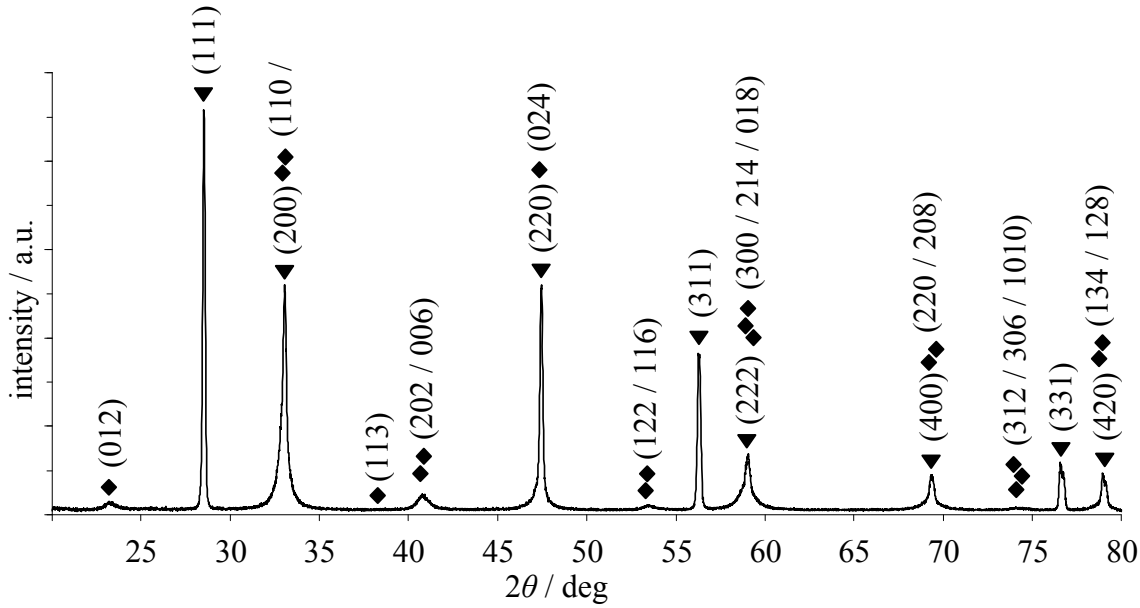

Figure 2: XRD pattern of a MOD derived nanoscaled $La_{0.6}Sr_{0.4}CoO_{3-\delta}$ thin film cathode on a $Gd_{0.1}Ce_{0.9}O_{1.95}$ electrolyte processed with ΔT = 3 K min^{-1}, T_{max} = 700 °C and t_{an} = 0 h. ♦ denotes the position of $La_{0.6}Sr_{0.4}CoO_{3-\delta}$ peaks [12] and ▼ those of $Ce_{0.9}Gd_{0.1}O_{1.95}$ [13].

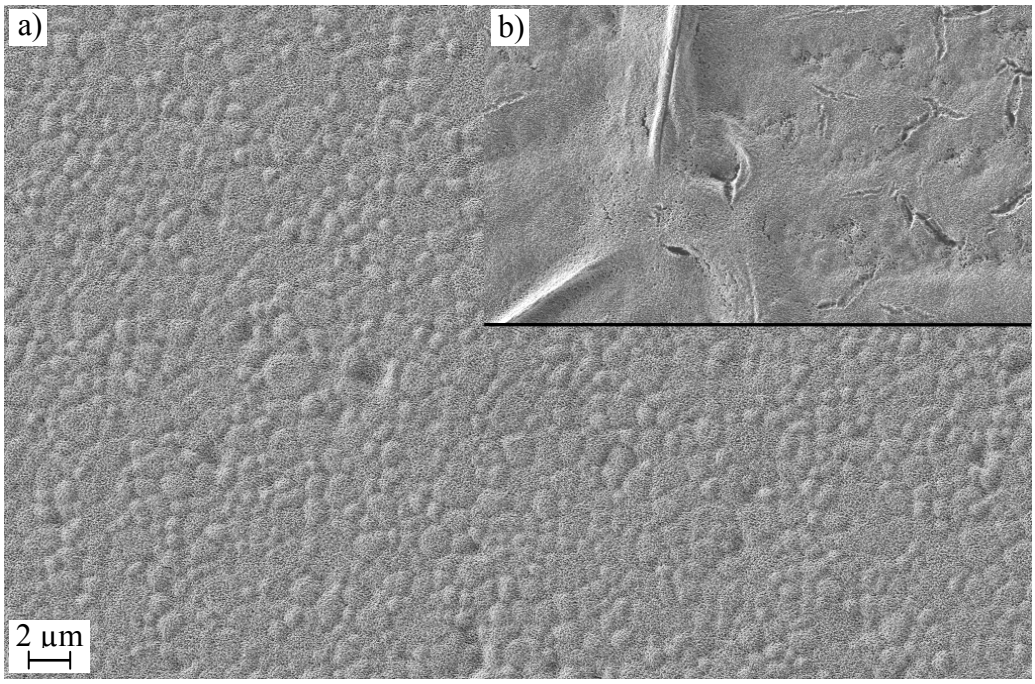

Figure 3: Low magnification SEM micrographs of thin film cathodes on a GCO electrolyte substrate prepared with the processing parameters a) ΔT = 3 K min^{-1}, T_{max} = 800 °C, t_{an} = 10 h and b) ΔT = rapid thermal annealing (RTA), T_{max} = 800 °C, t_{an} = 10 h. Thin film layers processed with a slow heating rate exhibited no cracks or areas of inhomogeneity over the whole substrate surface. The patterning of the layer is a result of the topography of the grains and grain boundaries of the electrolyte substrate. RTA led to a bulgy layer with cracks.

All samples prepared by MOD applying a slow heating rate of 3 K min^{-1} led to crack-free thin films with a nanoscaled microstructure as shown in Figure 3a). However, if the samples were processed with RTA, they exhibited a very inhomogeneous structure with bulges and cracks (Figure 3b)). The main focus within this project was on the slowly heated samples, as they exhibited a homogeneous microstructure. The RTA prepared samples are only included in this report to give an overview of the microstructures which can be derived by MOD technique.
Figure 4 depicts high-resolution SEM micrographs of the different surface morphologies of nanoscaled cathodes, processed with a slow heating rate of 3 K min^{-1}. Controlled by the maximum processing temperature and annealing time, cathodes with mean grain sizes ranging from 17 nm to 90 nm and porosities of up to 45 % were obtained. Both the smallest mean grain size and the highest porosity were determined for the sample calcined at 700 °C without further annealing (Figure 4 a)). A detailed compilation of the microstructural data can be found in Table 2.

Table 2: Microstructural properties of nanoscaled thin film cathodes prepared with ΔT = 3 K min^{-1}. $d_{mean,TEM}$ denotes the mean grain size determined by TEM analysis, $d_{mean,SEM}$ the mean grain size determined by SEM analysis. ε denotes the porosity determined by STEM tomography.

Processing of sample		$d_{mean,TEM}$	$d_{mean,SEM}$	ε
T_{max} (°C)	t_{an} (h)	(nm)	(nm)	(vol %)
700	0	17 ± 5	16.4 ± 7.82	45 ± 10
700	10	not determined	25.0 ± 11.4	not determined
700	100	28 ± 10	30.2 ± 14.1	not determined
800	0	29 ± 10	27.0 ± 10.6	17 ± 5
800	10	not determined	38.8 ± 18.8	not determined
800	100	90 ± 33	63.5 ± 33.5	not determined

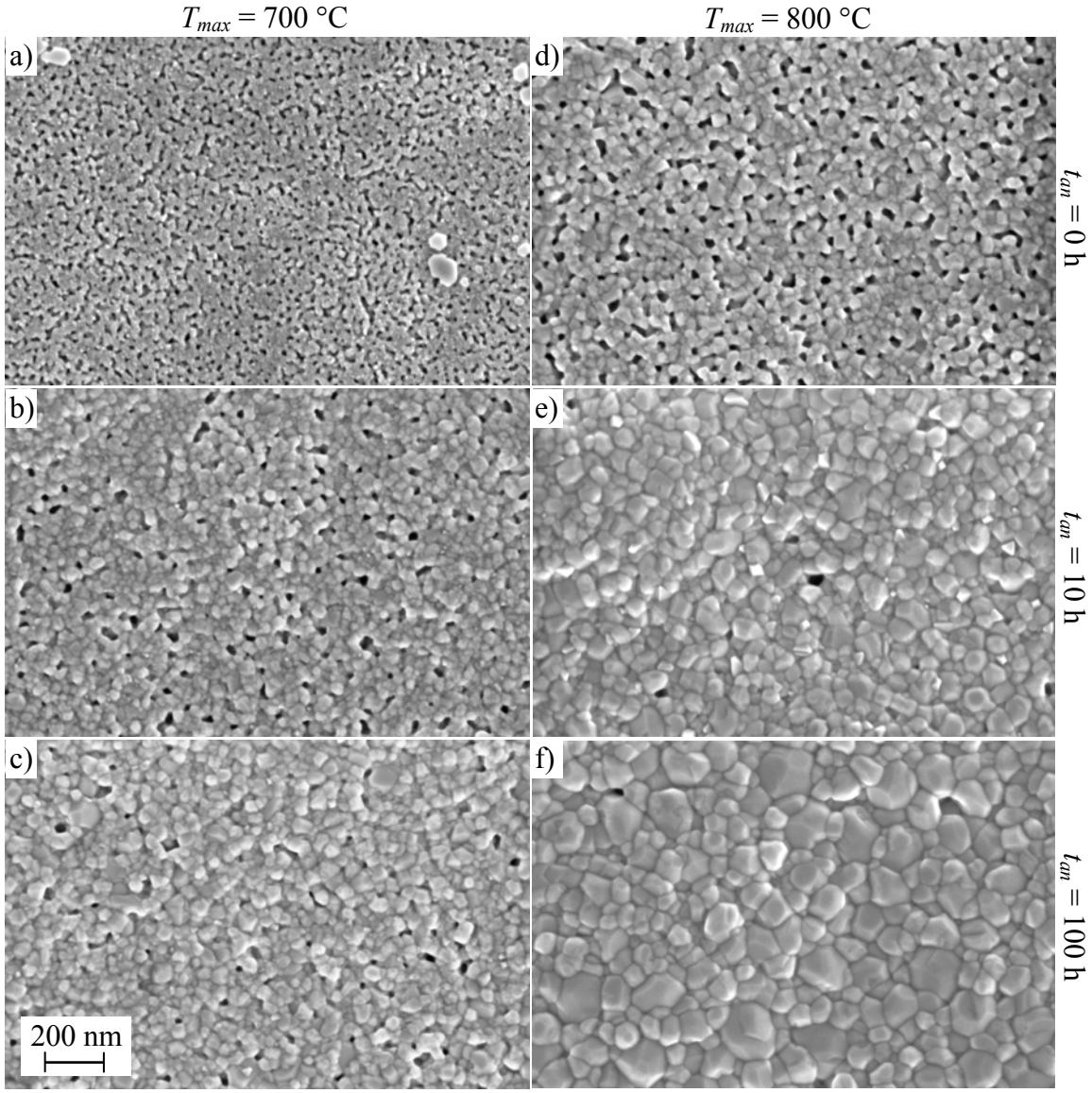

Figure 4: SEM surface micrographs of nanoscaled cathodes processed at 700 °C and 800 °C for up to 100 h (ΔT = 3 K min^{-1} for all samples).

The mean grain sizes determined with the two methods (SEM and TEM) are in good agreement. Only for large grain sizes, the results differ significantly. This is most likely the result of overlapping grains that partly cover each other – if observed from the surface – leading to an underestimation of the grain size by SEM surface analysis. In the following, particle sizes determined by TEM will be used. For those samples, where no TEM data is available, SEM derived data will be applied.

As expected, the grain size increases with increasing maximum processing temperature and with increasing annealing time. The porosity decreases with increasing maximum processing temperature and with increasing annealing time. One coating step resulted in an average layer thickness of approximately 200 nm.

The cross-sectional images in

Figure 5 a) and b) give a visual impression of the large range of grain sizes, which can be obtained by MOD. The two images represent the upper and lower bound in terms of porosity and particle size.

Figure *5* c) and d) depict thin film cathode samples processed with the same parameters as the samples in a) and b), respectively, except for the heating rate. Representative for all samples treated with rapid thermal annealing, these cathodes exhibited a dense surface layer with a high closed porosity underneath. We attribute this to a rapid heating of the coating's surface, which immediately formed a dense oxide surface layer. The gaseous decomposition products of the metal organics from the material underneath then lead to a high, closed porosity and large cavities beneath the dense surface layer. Grain size and porosity values could not be determined for these layers, as the layers are highly inhomogeneous.

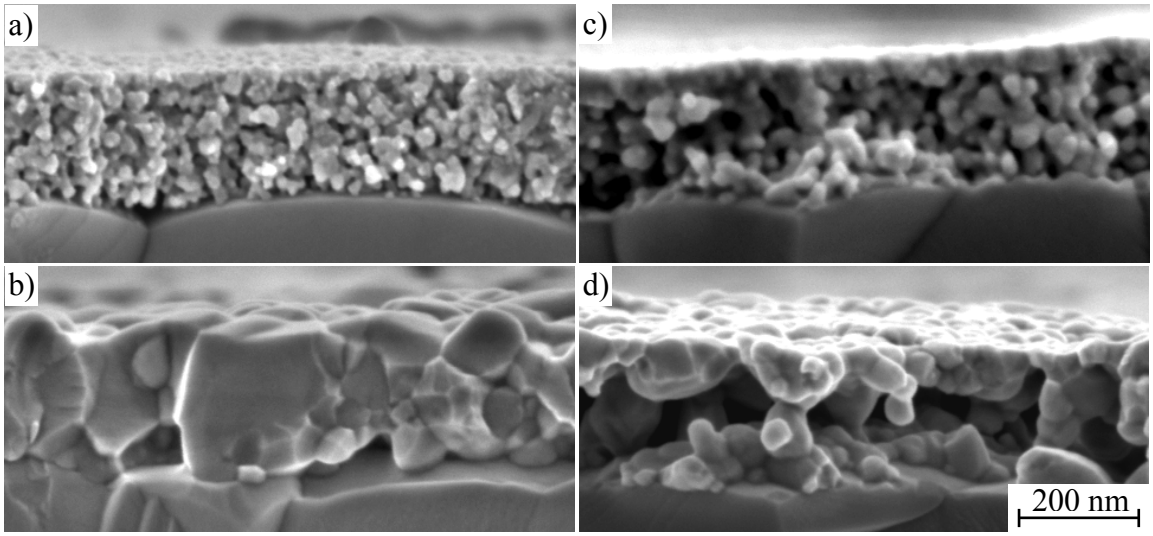

Figure 5: SEM micrographs of nanoscaled cathode cross-sections of samples processed at a) ΔT = 3 K min^{-1}, T_{max} = 700 °C, t_{an} = 0 h, b) ΔT = 3 K min^{-1}, T_{max} = 800 °C, t_{an} = 100 h, c) ΔT = RTA, T_{max} = 700 °C, t_{an} = 0 h and d) ΔT = RTA, T_{max} = 800 °C, t_{an} = 100 h.

3.3 Electrochemical characterization

Influence of the current collector on the cathode performance

Before analyzing the electrochemical characteristic of nanoscaled cathodes, possible sources of error must be carefully considered. These could be, for example, possible contributions of the current collector layer to the cathodic electrochemical reaction, or current constrictions arising from insufficient contacting of the nanoscaled cathodes. The latter arise, if the contact spacings are too large. This would be the case, if the thin film cathodes were contacted by a gold mesh only, which is commonly used for contacting SOFC cathodes in a measuring setup. The low cathode film thickness would then lead to a low lateral electronic conductivity in between the contact points of the gold mesh nods (distance ≈ 250 µm) resulting in areas of reduced activity. To avoid this, a current collector layer (CCL) of µm-sized LSC particles (d_{50} ≈ 1.8 µm) was applied on top of the thin-film cathodes. To evaluate possible influences of this current collector, the polarization losses of a cathode made of the current collector layer only were determined experimentally and theoretically by an appropriate model.

a) For the calculation of the electrochemical characteristic of CCL in terms of area specific polarization losses, a 1D model by Adler et al. [15;16] for a semi-infinite porous mixed conducting cathode with a fast ionic transport, a high electronic conductivity and no gas phase limitations was applied. Our LSC type current collector layer fulfills these requirements [15]. The necessary geometry related parameters, solid phase tortuosity $\tau = 1.75$ and volume specific surface area $a = 1.42 \cdot 10^6$ m^{-1}, were calculated with the aid of a 3D finite element method (FEM) microstructure model, which was developed at our institute (Rüger et al. [17]). In addition, a geometry correction

term was applied, which was determined by a focused ion beam (FIB) tomography 3D reconstruction of a real electrode structure, which was performed at our institute as well [18]. It needs to be noted, that these numbers were derived with the assumption, that the CCL layer exhibits a microstructure similar to a sintered electrode structure, which is not the case here, as the current collector layer is used in an unsintered state. Therefore, the derived values for the specific surface area and the tortuosity can only serve as an estimate. The calculations predict an area specific resistance associated with the cathodic polarization loses of ASR_{calc} = 1.44 Ωcm² at 600 °C.
b) Experimentally, a twice as high value was determined with ASR_{meas} = 2.85 Ωcm² at 600 °C. For this, a cathode made of the LSC current collector layer only was electrochemically characterized in a symmetric setup. The current collector was applied by screen printing as a 30 µm thick layer and was characterized in an unsintered state on a GCO pellet in stagnant air. The comparably high polarization losses measured for this type of cathode can be attributed to the poor interface between the cathode and the electrolyte and to not sintered cathode particles.
As the measured value is more than 100 times higher and the calculated value is still more than 60 times higher than the lowest value measured on a nanoscaled thin film cathode (ASR_{min}) and since they are still 17 and 9 times higher than the highest (ASR_{max}), respectively, the influence of the current collector on the electrochemical performance can be considered negligible for such high performance cathodes (see Table 3).

Table 3: Area specific polarization resistance values of a µm-scaled LSC current collector layer determined by 1D model calculations (ASR_{calc}) and EIS measurement (ASR_{meas}) in comparison to the highest and lowest area specific resistance values measured on nanoscaled cathodes (ASR_{max} and ASR_{min}).

µm-scaled LSC CCL		nanoscaled thin film cathodes	
ASR_{calc} / Ωcm²	ASR_{meas} / Ωcm²	ASR_{min} / Ωcm²	ASR_{max} / Ωcm²
1.44	2.85	0.023	0.165

Electrochemical impedance spectroscopy analysis

Electrochemical characterization was performed by means of electrochemical impedance spectroscopy (EIS) on a symmetrical cell setup. The active cell area of the cathodes was 1 x 1 cm² and the test cells were contacted with a gold mesh (>99.99% Au, 1024 meshes.cm^{-2}, 0.06 mm wires), leading to a homogeneous current distribution over the electrode. EIS measurements were carried out under open circuit conditions in stagnant ambient air in temperature steps of 25 K from 400 to 600 °C using a Solartron 1260 frequency response analyzer in a frequency range of $10^{-1} < f < 10^{6}$ Hz. The impedance data were then analyzed by calculating and analyzing the corresponding distribution function of relaxation times (DRTs) [19] and CNLS fitting (Z-View® software v2.8, Scribner Associates Inc.).
Figure 6 depicts a comparison of the results form this study to the results from D5.2, which were summarized by Peters et al. in [6], and which were obtained for MOD derived nanoscaled $La_{0.5}Sr_{0.5}CoO_{3-\delta}$ thin film cathodes processed at T_{max} = 900 °C. In comparison, samples processed according to Table 1 exhibited a significantly higher performance, except for the sample annealed at 800 °C for 100 h. At 600 °C polarization losses range from 0.023 to 0.165 Ωcm^2. The lowest value was determined for the cathode with the highest porosity of ε = 45 % and the smallest average grain size of d_{mean} = 17 nm (see Figure 3a) and 4a)), which therefore exhibited the largest surface area for the oxygen surface exchange reaction.
All cathodes exhibited nearly the same activation energy of E_a = 1.41 ± 0.03 eV. As the cathodic reaction was determined to be surface controlled for these thin film cathodes [20], this value is in good agreement with the activation energy of E_a = 1.3 ± 0.1 eV reported for the resistance associated with the oxygen surface exchange of $La_{0.6}Sr_{0.4}CoO_{3-\delta}$ [4]. Peters et al. [6] determined their $La_{0.5}Sr_{0.5}CoO_{3-\delta}$ thin film cathodes to be surface exchange controlled as well, with

E_a = 1.07 eV. In agreement with the trend, that the activation energy of the surface exchange coefficient decreases with increasing Sr-content [21], a lower activation energy was observed.

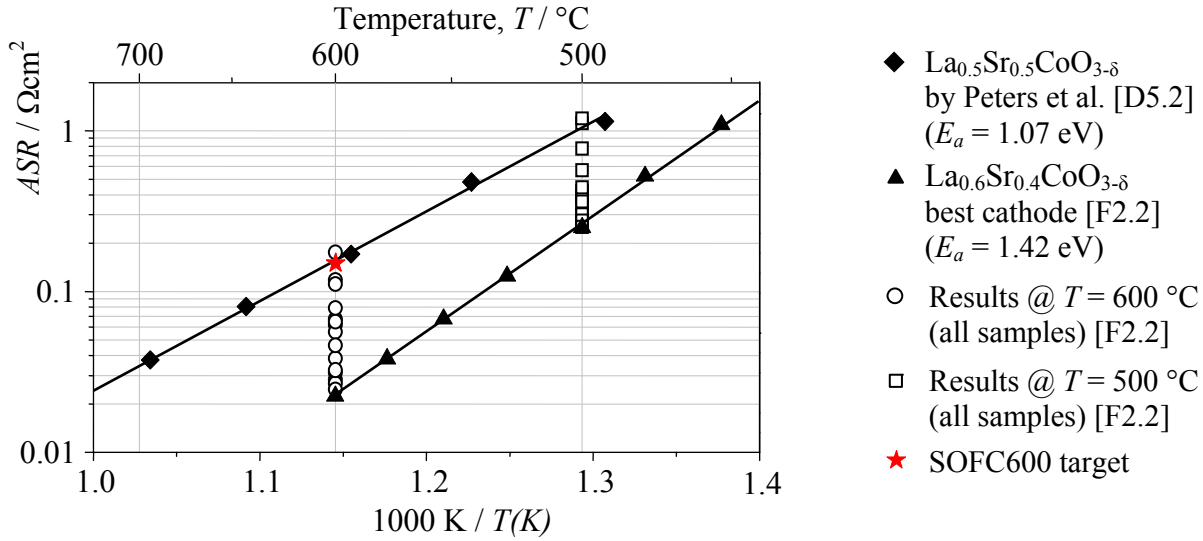

Figure 6: Arrhenius plot of the results D5.2 (♦) (Peters et al. [6]) and the best nanoscaled $La_{0.6}Sr_{0.4}CoO_{3-\delta}$ thin film cathode (T_{max} = 700 °C, t_{an} = 0 h and ΔT = 3 K min^{-1}) measured in this study (▲). The open symbols represent results from all prepared samples measured at 500 °C (□) and 600 °C (○). Benchmark: target value of the SOFC600 project (EU project, FP6-2004-Energy-3, contract no. 020089)

The results of the samples prepared with the slow heating rate (3 K min^{-1}) are displayed in more detail in Figure 7. As depicted in Figure 7 a), for a maximum processing temperature of 700 °C most of the grain growth occurred within the first 10 hours. After another 90 hours, no significant change was observed. However, as the porosity decreased with increasing annealing time, the surface area available for the electrochemical reaction was reduced, leading to an increase of the area specific polarization losses (Figure 7 b)). According to Adler et al. [15] the ASR_{chem} is inversely proportional to the volume specific surface area, if the cathode is surface exchange controlled. This effect is even more obvious if the samples prepared at 700 °C with 10 h and 100 h of annealing are compared to the sample prepared at 800 °C with 0 h of annealing). The grain sizes are about the same, however the ASR_{chem} is significantly lower for the latter sample. This is attributed to the comparably large open porosity. Sample annealing at 800 °C for 10 h and 100 h leads to a continuing grain growth and dense films, reducing the sites for the cathodic reaction to the comparably small surface area of the cathode film surface. The resulting losses are therefore significantly higher.

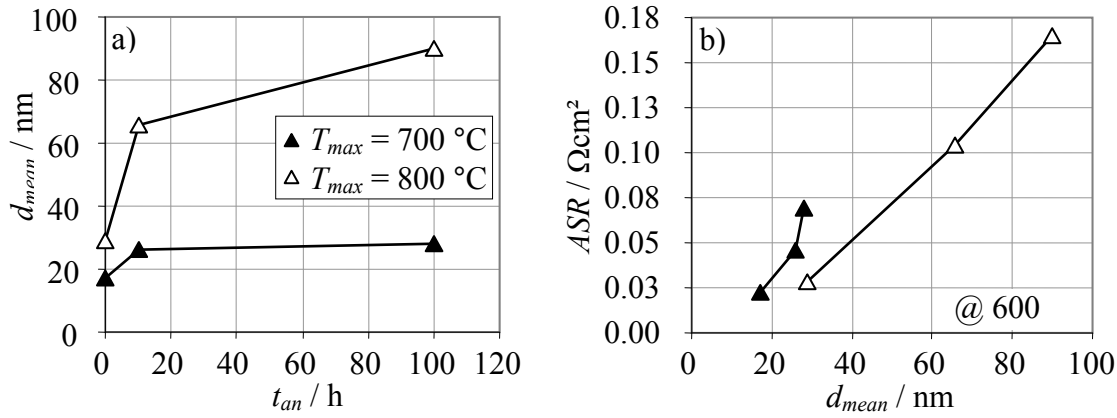

Figure 7: The two graphs depict a) the microstructure analysis results and b) the performance analysis results of the samples prepared with the slow heating rate (ΔT = 3 K min^{-1}) in more detail. Graph a) shows

the mean grain size (d_{mean}) with respect to the annealing time. Graph b) plots the measured area specific polarization losses at 600 °C over the mean grain size.

In Figure 8, the polarization losses measured in the present study are compared to results from the previous projects D5.2 [6] and D6.3 [22] and other values reported in literature for (La,Sr)$CoO_{3-\delta}$ type perovskites [15;23;24] and other promising candidate materials, such as (Ba,La,Sr)(Co,Fe)$O_{3-\delta}$ (BLSCF) [22] or (La,Sr)(Co,Fe)$O_{3-\delta}$ (LSCF) [22;25] type perovskites. For (La,Sr)$CoO_{3-\delta}$, it is unambiguously shown, that reducing the particle size from the µm to the nm regime drastically reduces the polarization losses of about factor 50. This comparison also reveals that $La_{0.6}Sr_{0.4}CoO_{3-\delta}$ is a very promising candidate for intermediate or low temperature operation, as it outperforms other material compositions, applied as nm-scaled cathodes or nm-scaled composite cathodes (combination of cathode material and electrolyte material, such as GCO). Only an LSCF cathode by Baqué et al. [25] exhibits lower polarization losses at temperatures of 400 – 500 °C. However, as this cathode shows a very unusual – not Arrhenius type – temperature activation, this cathode type seems to have severe temperature stability problems, which relativise these results.

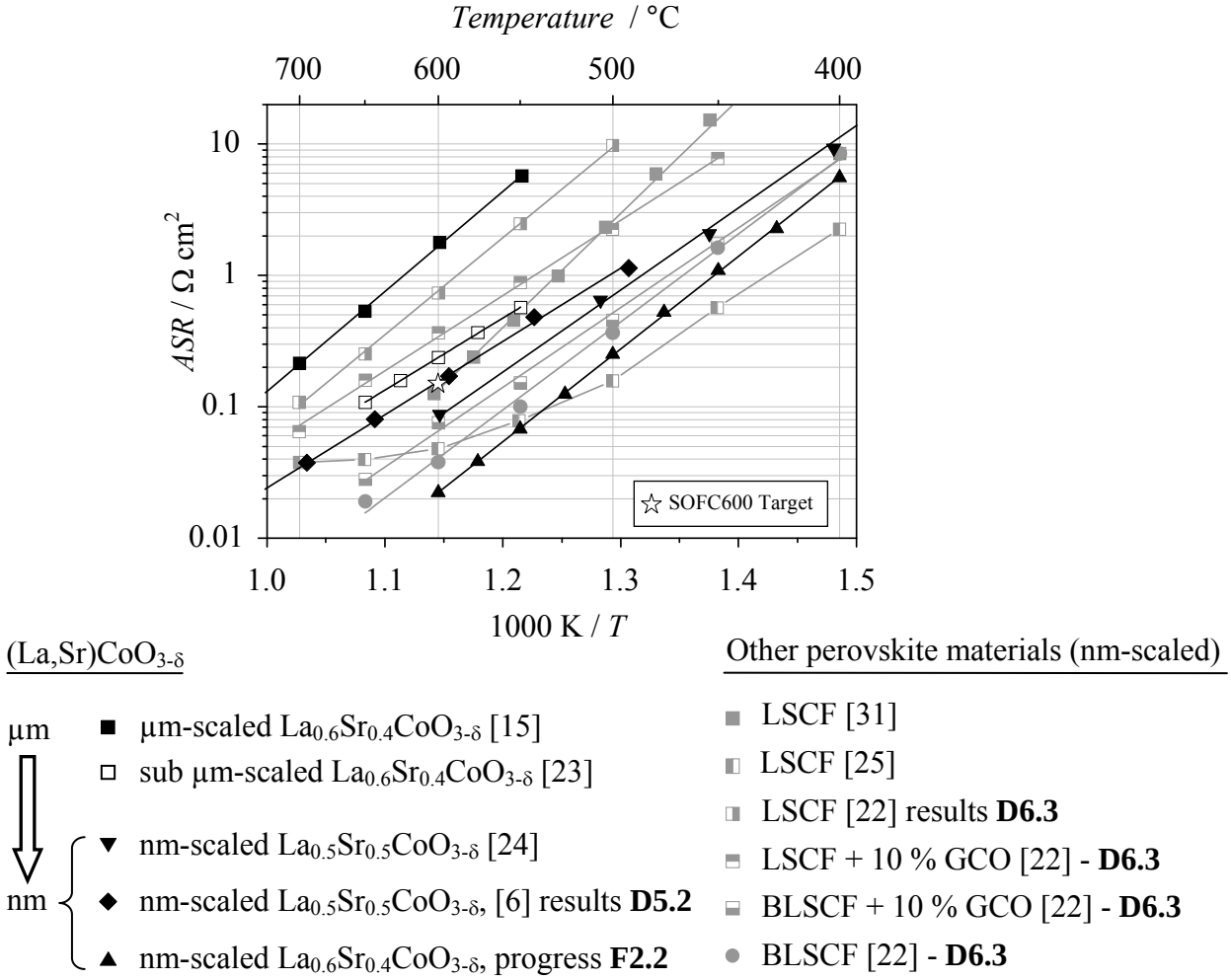

Figure 8: Comparison of different sized (La,Sr)$CoO_{3-\delta}$ cathodes (black symbols) to other promising perovskite materials, such as (La,Sr)(Co,Fe) $O_{3-\delta}$ (LSCF) or (Ba,La,Sr)(Co,Fe)$O_{3-\delta}$ (BLSCF) applied as nanoscaled cathodes or nanoscaled (GCO-)composite cathodes (grey symbols). For (La,Sr)$CoO_{3-\delta}$, reducing the particle size from the µm to the nm regime leads to a reduction of the polarization losses of factor 50. The addition of Ba or Fe does not lead to cathodes with increased performance.

3.4 Theoretical considerations

As the measured polarization resistances are extremely low, the question arose, if it is the nanoscale of the microstructure that enables such low values, or if the MOD processing route leads to LSC with enhanced catalytic properties. A comparison of measured data with theoretically obtained values applying 1-dimensional continuum modeling [16] clarified this aspect. The general equation was simplified for the case of a thin film cathode, where the theoretical penetration depth of the electrochemical reaction δ exceeds the electrode thickness. In this case, the entire surface area of the cathode is utilized and polarization losses are related to the surface exchange only [15].
Apart from material related parameters, such as the surface exchange coefficient k^* and the vacancy diffusion coefficient D_v, which were taken from literature [15], also geometry related parameters were input to the model. These are for example the solid phase tortuosity τ and the volume specific surface area a_1, which were again calculated with the aid of the 3D FEM microstructure model mentioned above [17]. Furthermore, in a second data set, the volume specific surface area was modified with the FIB-reconstruction derived correction term ($a_2 = 1.83 \cdot a_1$) which was already mentioned above [18].
Table 4 lists the details of two cathodes of different particle size (*ps*) for which the calculations were made. The cathodes were of thickness $l_{Cat} = 210$ nm with an estimated porosity of $\varepsilon = 0.3$ and a resulting tortuosity of $\tau = 1.4$.

Table 4: Two samples of different particle size were chosen for comparing measured (EIS) and calculated ASR values (at 600 °C). For each particle size, δ (penetration depth of the electrochemical reaction) and ASR values were determined for two volume specific surface areas a_1 (3D-FEM) and a_2 (FIB reconstruction corrected).

ps nm	a_1 1/m	a_2 1/m	δ_{a1} nm	δ_{a2} nm	ASR_{a1} Ω·cm²	ASR_{a2} Ω·cm²	ASR_{EIS} Ω·cm²
15	$8.17 \cdot 10^7$	$1.49 \cdot 10^8$	276	204	0.22	0.11	0.023
30	$4.08 \cdot 10^7$	$7.46 \cdot 10^7$	390	288	0.43	0.23	0.028

For all cases, the penetration depth δ is greater or equal to the cathode thickness. As the diffusion coefficient (D_v), which was used for these calculations, is low and the surface exchange coefficient is high – compared to others reported in literature [12;21;26-29] (in some cases the data have been extrapolated assuming Arrhenius behavior for comparison) – this value can be regarded as a minimum penetration depth. The actual penetration depth might actually be significantly higher.
The resulting polarization resistances are more than 5 times higher than the measured values, even though a comparably high surface exchange coefficient has been chosen. The high performance of the nanoscaled cathodes can thus not solely be explained by an enlargement of the inner surface area, resulting from a nanoscaled microstructure, as suggested in the conclusions of project D5.2 [6]. Therefore, it is concluded that nanoscaled LSC prepared by MOD must exhibit enhanced catalytic properties for the oxygen surface exchange reaction, significantly higher than those of LSC bulk material prepared by conventional methods such as solid state reaction or a glycine–nitrate route.
A backwards calculation, yielding the value for the surface exchange coefficient, leads to $k^* = 3.16 \cdot 10^{-6}$ cm/s (assuming ps = 15 nm, $a = 1.49 \cdot 10^8$ m^{-1}, $l_{Cat} = 210$ nm, $ASR_{chem} = 0.023$ Ω·cm²), calculated with $c_{mc} = 85530$ mol/m³ [27]. For comparison, the value obtained by Adler et al. [15] is by a factor of 5 smaller with $k^* = 6.20 \cdot 10^{-7}$ cm/s. The cause for this distinct improvement has not been identified and understood yet, but recent results of TEM performed chemical analyses revealed nanoscaled Co_3O_4 precipitates on the cathode thin film surface, which may act catalytically to enhance the surface exchange of oxygen [30].

Simulations with our 3D FEM model [17] lead to similar results as the 1D model without the TEM correction factor (see Figure 9). However, it is clearly visible, that the 1D model slightly underestimates the polarization losses, as, for example, current constrictions within the electrolyte are not taken into account by this rather simple model. For the 3D FEM calculations, a porosity of $\varepsilon = 0.3$ was applied as well. It needs to be noted, that the porosity does not exactly match the one measured by 3D STEM tomography, as these results were obtained recently. However, as the error resulting from this deveation is rather small (~20 % if the porosity is 0.5 instead of 0.3) the conclusion remains unaffected. In the next reporting period, an updated data set will be available.

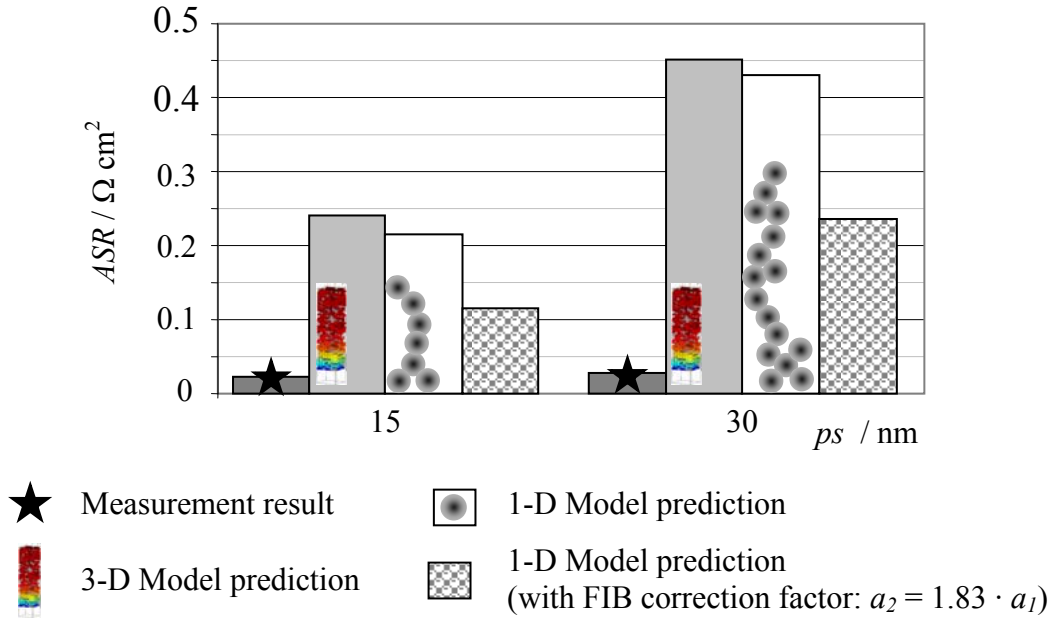

Figure 9: Comparison of the results for T = 600 °C obtained by EIS measurements, 3D-FEM microstructure model simulations, 1D model calculations and 1D model calculations applying a FIB-reconstruction derived correction factor for determining the volume specific inner surface areas. The calculations were performed for a particle size of 15 and 30 nm, a porosity of $\varepsilon = 0.3$ and, in the case of the 1D model, a tortuosity $\tau = 1.4$.

4. Summary and Outlook

In the present study, nanostructured cathodes made of the perovskite material $La_{0.6}Sr_{0.4}CoO_{3-\delta}$ were prepared and characterized, which exhibited outstanding performances with polarization losses as low as 0.023 Ωcm^2. For the first time, a variation of the microstructure on the nanometer scale was systematically studied, with the focus on the correlation of the microstructure and the reaction kinetics in terms of area specific resistance. By applying different processing parameters, such as maximum processing temperature, heating rate and annealing time, a wide span of truly nanoscaled microstructural features, such as nanoscaled porosity in the range of 0 – 45 % and grain sizes from 17 to 90 nm, was obtained. The high volume specific inner surface area, which is a result of small particles in combination with a high open porosity, is the major feature, which enables such low polarization losses. Going from "micro" (particle sizes in the range of 1 – 2 μm) to "nano", a significant reduction in area specific resistance of factor 50 was demonstrated.
The experimentally obtained results were tried to be interpreted by modelling, based on material related parameters determined on bulk samples. However, it was not possible to explain the exceptionally good results applying these parameters, neither with a 1D analytical model, nor by a detailed 3D FEM microstructure model. It is concluded, that nanoscaled MOD derived LSC exhibits enhanced catalytic properties, which might, at least in parts, be explained by nano-particulate Co_3O_4 precipitates on the thin film cathode surface, as revealed by a recent TEM investigation. A significant contribution of the current collector layer to the cathodic electrochemical reaction could be ruled out.
Furthermore, the results of the present study opened up a whole new aspect to nanoscaled cathodes made by MOD derived LSC, as they did not only exhibit excellent performances at temperatures of 600 °C (6x better than the target value of the European Union project SOFC600), but also revealed very promising results at temperatures as low as 500 °C – a typical target operation temperature of μ-SOFCs. μ-SOFCs, fabricated on a chip, are currently investigated as a potential battery replacement for notebooks or related devices.

With the results of this work, we have been able to further increase the performance of the nanostructured cathodes by a factor of 5, compared to the results obtained in the previous subprojects D5.2 and D7.2. Depending on microstructure, polarization losses between 0.023 – 0.165 Ωcm^2 at 600 °C were achieved, which are the lowest values reported in literature. Several measurements lead to this improvement: chemically compatible material choice for the electrolyte substrate, different sol chemistry of the metal organic deposition process and decisively modified processing parameters with maximum processing temperatures as low as 700 °C.

Consequently, future work must focus on a detailed understanding of the surface chemistry of nanoscaled LSC thin film cathodes, which facilitates the oxygen reduction reaction. This interaction with the gas phase is crucial for the goal to make precise predictions with our 3D FEM microstructure model. Especially the interaction of impurities contained in ambient air (e.g. H_2O or CO_2) with the cathode material, with regard to the surface exchange of oxygen, is of great interest, as due to the high surface-to-volume ratio, these electrodes and their reaction kinetics are highly sensitive to poisoning or other sources of degradation. This feature opens up an all new possibility to study such effects on a completely different sensitivity level.
With a detailed understanding of the surface chemistry it is also expected that new ways of improving nanoscaled LSC cathodes will be identified. Motivated by preliminary results, a deliberate fine-tuning of the kinetic properties of nanoscaled cathodes by a systematic surface modification with nano-particulate binary oxides (e.g. Co_3O_4 or SrO) could be an easy but powerful way to significantly enhance the surface exchange kinetics of nanoscaled LSC or other types of cathodes.

References

- own work with complete titles -

[1] A. Weber and E. Ivers-Tiffée, "Materials and concepts for solid oxide fuel cells (SOFCs) in stationary and mobile applications", *J. Power Sources* **127**, pp. 273-283 (2004).

[2] E. Ivers-Tiffée, A. Weber and D. Herbstritt, "Materials and technologies for SOFC-components", *Journal of the European Ceramic Society* **21**, pp. 1805-1811 (2001).

[3] D. Herbstritt, A. Weber, U. Guntow, G. Müller and E. Ivers-Tiffée, "Cathode-Performance: Influence of MOD-Intermediate Layer and Electrolyte Surface Enlargement", in A. J. McEvoy (Ed.), *Proceedings of the 4th European Solid Oxide Fuel Cell Forum* **2**, pp. 697-706 (2000).

[4] F. S. Baumann, J. Fleig, G. Cristiani, B. Stuhlhofer, H. U. Habermeier and J. Maier, *J. Electrochem. Soc.* **154**, p. B931-B941 (2007).

[5] J. Maier, *Journal of the European Ceramic Society* **24**, pp. 1251-1257 (2004).

[6] C. Peters, A. Weber and E. Ivers-Tiffée, "Nanoscaled $(La_{0.5}Sr_{0.5})CoO_{3-\delta}$ Thin Film Cathodes for SOFC Application at 500°C < *T* < 700°C", *J. Electrochem. Soc.* **155**, p. B730-B737 (2008).

[7] D. Beckel, A. Bieberle, A. Harvey, A. Infortuna, U. P. Muecke, M. Prestat, J. L. M. Rupp and L. J. Gauckler, *J. Power Sources* **173**, pp. 325-345 (2007).

[8] J. Hayd, U. Guntow and E. Ivers-Tiffée, "Electrochemical performance of nanoscaled $La_{0.6}Sr_{0.4}CoO_{3-\delta}$ as intermediate temperature SOFC cathode", *ECS Trans.* **28**, pp. 3-15 (2010).

[9] J. Hayd, U. Guntow and E. Ivers-Tiffée, "Nanoscaled $La_{0.6}Sr_{0.4}CoO_{3-\delta}$ as intermediate temperature SOFC cathode: Microstructure and electrochemical performance", *J. Power Sources* **10**, pp. 106-112 (2010).

[10] L. Dieterle, D. Bach, R. Schneider, H. Störmer, D. Gerthsen, U. Guntow, E. Ivers-Tiffée, A. Weber, C. Peters and H. Yokokawa, "Structural and chemical properties of nanocrystalline $La_{0.5}Sr_{0.5}CoO_{3-\delta}$ layers on yttria-stabilized zirconia analyzed by transmission electron microscopy", *Journal of Materials Science* **43**, pp. 3135-3143 (2008).

[11] P. Gilbert, *Journal of Theoretical Biology* **36**, pp. 105-117 (1972).

[12] R. H. E. van Doorn, Dissertation, University of Twente (1996).

[13] G. Brauer and H. Gradinger, *Zeitschrift für Anorganische und Allgemeine Chemie* **276**, pp. 209-226 (1954).

[14] S. B. Adler, *Chemical Reviews* **104**, pp. 4791-4843 (2004).

[15] S. B. Adler, *Solid State Ionics* **111**, pp. 125-134 (1998).

[16] S. B. Adler, J. A. Lane and B. C. H. Steele, *J. Electrochem. Soc.* **143**, pp. 3554-3564 (1996).

[17] B. Rüger, A. Weber and E. Ivers-Tiffée, "3D-Modelling and Performance Evaluation of Mixed Conducting (MIEC) Cathodes", *ECS Trans.* **7**, pp. 2065-2074 (2007).

[18] J. Joos, B. Rüger, T. Carraro, A. Weber and E. Ivers-Tiffée, "Electrode Reconstruction by FIB/SEM and Microstructure Modeling", *ECS Trans.* **28**, pp. 81-91 (2010).

[19] H. Schichlein, A. C. Müller, M. Voigts, A. Krügel and E. Ivers-Tiffée, "Deconvolution of electrochemical impedance spectra for the identification of electrode reaction mechanisms in solid oxide fuel cells", *Journal of Applied Electrochemistry* **32**, pp. 875-882 (2002).

[20] C. Peters, A. Weber and E. Ivers-Tiffée, "Nanoscaled $(La_{0.5}Sr_{0.5})CoO_{3-\delta}$ Thin Film Cathodes for SOFC Application at 500°C < *T* < 700°C", *J. Electrochem. Soc.* **155**, p. B730-B737 (2008).

[21] A. V. Berenov, A. Atkinson, J. A. Kilner, E. Bucher and W. Sitte, *Solid State Ionics* **181**, pp. 819-826 (2010).

[22] A. J. Darbandi and H. Hahn, *Solid State Ionics* **180**, pp. 1379-1387 (2009).

[23] F. P. F. van Berkel, S. Brussel, M. van Tuel, G. Schoemakers, B. Rietveld and P. V. Aravind, in J. A. Kilner (Ed.), *Proceedings of the 7th European Solid Oxide Fuel Cell Forum*, p. 1 (2006).

[24] S. Wang, J. Yoon, G. Kim, D. Huang, H. Wang and A. J. Jacobson, *Chemistry of Materials* **22**, pp. 776-782 (2010).
[25] L. Baqué, E. Djurado, C. Rossignol, D. Marinha, A. Caneiro and A. Serquis, *ECS Trans.* **25**, pp. 2473-2480 (2009).
[26] M. H. R. Lankhorst, Dissertation, University of Twente (1997).
[27] M. Søgaard, P. V. Hendriksen, M. Mogensen, F. W. Poulsen and E. Skou, *Solid State Ionics* **177**, pp. 3285-3296 (2006).
[28] T. Inoue, J. Kamimae, M. Ueda, K. Eguchi and H. Arai, *J. Mater. Chem.* **3**, pp. 751-754 (1993).
[29] R. Ganeshananthan and A. V. Virkar, *J. Electrochem. Soc.* **153**, p. A2181-A2187 (2006).
[30] L. Dieterle, P. Bockstaller, D. Gerthsen, J. Hayd, E. Ivers-Tiffée and U. Guntow, "Microstructure of Nanoscaled $La_{0.6}Sr_{0.4}CoO_{3-\delta}$ Cathodes for Intermediate-Temperature Solid Oxide Fuel Cells", *Adv. Func. Mat.* (2010) in press.
[31] D. Marinha, J. Hayd, L. Dessemond, E. Ivers-Tiffée, E. Djurado, "Performance of LSCF double-layer cathode films for IT-SOFC", *Journal of Power Sources* (2010) in press.